HETEROCYCLES, Vol. 102, No. 5, 2021, pp. 825 - 849. © 2021 The Japan Institute of Heterocyclic Chemistry
Received, 13th August, 2020, Accepted, 2nd October, 2020, Published online, 27th October, 2020
DOI: 10.3987/REV-20-939

ATTRACTIVE ORGANIC COCRYSTAL MATERIALS IN OPTICS

Xiao Han,* Linyu Wang, and Gaiqing Xi

College of Chemical Engineering & Material, Hebei Key Laboratory of Heterocyclic Compounds, Handan University, Handan 056005, Hebei, China, E-mail: hanxiao2007510806@126.com

Abstract – Since the beginning of this century, organic molecule solid material, one of favorable choices for constructing high-performance optoelectronic devices/circuits, has showed the impressive perspective in organic optoelectronics. Especially, because of the long-range order, absent grain boundary and extremely low defect density, organic single-crystal material support a great platform for fundament and application researches. Herein, cocrystal engineering, one simply collaborative strategy, shows offers the unique advantages, involving facile and low-cost synthesis procedure, easily achieving rare and multifunctional properties, tunable structure, morphology and size. It is extremely suitable to construct functional organic molecule solid material, especially novel multifunctional organic single-crystal materials. In this mini review, a overview of organic cocrystal is presented to introduce its attractive future in optics, such as OFET, lasing, nonlinear optics, optical waveguide material, stimuli-responsive material and other potential applications.

CONTENTS

1. Introduction
2. The basic introduction of organic cocrystal
3. Luminescent organic cocrystals
4. Application of organic cocrystal in OLET and lasing
5. Application of organic cocrystal in nonlinear optical and optical waveguide material
6. Application of organic cocrystal in stimuli-responsive material and other potential applications
7. Conclusions

1. INTRODUCTION

Over the past decades, exploring the functional molecular material has attracted obvious interest, especially organic single-crystal material.[1-4] For such material, several issues should be deeply understood for basic research and application, including requirements for high-quality crystals, adjustment of crystal functions and habits, and optimization of device configuration and interface contacts. Among these, organic cocrystal material was one of the shinning stars,[2-4] because cocrystal engineering could support one simply collaborative strategy for fabricating new functional organic single-crystal materials. Actually, although. Wöhler invented the first cocrystal in 1844, named quinhydrone, Schmidt and Snipes first mentioned the concept of "cocrystal" until 1967.[5] Since the highly conducting cocrystal tetrathiafulvalene-7,7,8,8-tetracyanoquinodimethane (TTF–TCNQ)[6] was found in 1973, cocrystal engineering gained increasing attentions for these potential applications in organic optoelectronics.[7] Encouraged by this example, cocrystal could serve as a composite to give the exploration of new and charming properties a chance, which might be far beyond the capability of single-component material. For example, dielectric response[8] nonlinear optics[9] and circularly polarized luminescence (CPL)[10] were observed in cocrystals by the rational heterosynthon method, which was absent in their constituents. On the other hand, cocrystal engineering opens up one simple way to achieve new organic multifunctional solid-state materials.[11] Recently, this bottom-up supramolecular assembly strategy provides the opportunity to accelerate the investigations of organic functional materials, where the exciting results showed the attractive future in different areas, such as room-temperature ferroelectricity,[12] ambipolar charge carrier transportation,[13] room temperature phosphoresce,[14-16] stimuli-responsiveness,[17-20] optical waveguide,[21] organic laser,[22] photovoltaics,[23] near-infrared photothermal (PT) conversion and imaging[24] and pharmaceutics.[25] Since 2012, there are some excellent reviews about the synthesis techniques/methods of organic cocrystals,[2,3,26-28] cocrystals for organic electronics[29,30] and field-effect transistors.[4] Herein, in this mini review, the overview of organic cocrystal will focus on the potential applications in optic area.

2. THE BASIC INTRODUCTION OF ORGANIC COCRYSTAL

The concept "cocrystal" was firstly put forward by Schmidt and Snipes in 1967, which was more than 120 year after the discovery of first cocrystal. Interestingly, the definition of organic cocrystal was a long-standing controversy, and the scientific discussions among crystallographers had never stopped until 2012. In that year, cocrystal was defined as crystalline solid consisting of two or more different molecules in a lattice.[31] As we know, for organic material, crystallization is the inherently purifying process, which can accomplish the long-range order, absent grain boundary and extremely low defect density. However, bringing two or more than two kinds of organic molecules into one crystal to achieve multifunction

always is a careful process, which needs deliberate design and action. Firstly, for the clear interaction mechanism and principles during co-crystallization, the complementary recognition of chemical groups from different molecules should be realized in the supramolecular synthesis route to cocrystal. It is vital to properly select the molecules for efficient co-crystallization[32] and to make various conformers structurally match, co-assemble and crystallize together.[33] Secondly, the relationships between crystal structure and performance is another key to the modulation of cocrystal properties.[34,35] Thirdly, to design and control stoichiometric ratio, molecular stacking mode, orientation, morphology and phase of cocrystals is an effective tuning of its function.[36] According to these considerations, enormous cocrystals have been generated by one or more non-covalent interaction (Scheme 1), such as charge-transfer (CT) interaction, aromatic attraction (π-π packing), halogen-bond and hydrogen-bond. Interestingly, the stabilities and properties of resulting cocrystals are also distinctly influenced by the dominant self-assembly driving force (noncovalent interaction).[37,38]

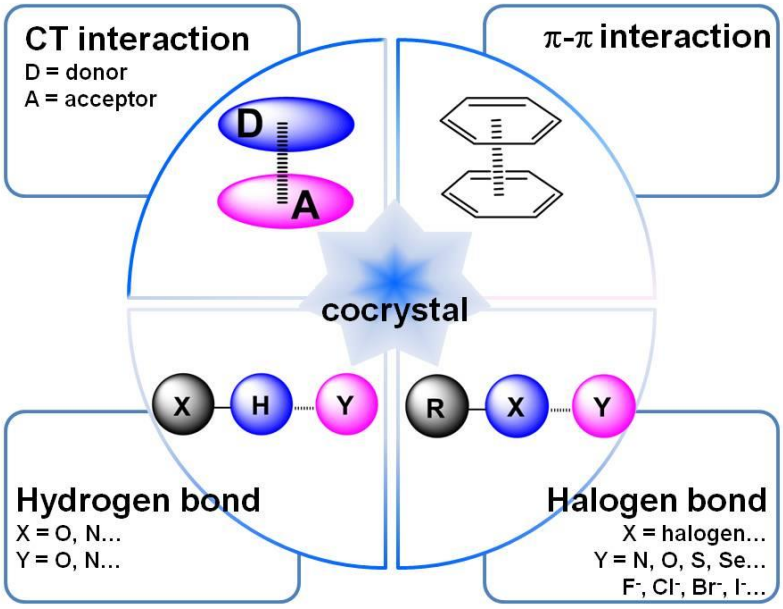

Scheme 1. The brief representations of the driving force for cocrystal formation

In present researches,[28] CT interaction is one of the most common driving force to form organic cocrystals. For example, when a strong acceptor TCNQ or TCNB assembled with an suitable donor, such as TTF, perylene, or pyrene, such interaction would dominate the cocrystal formation.[7,24] Commonly, the strength of CT interaction depends on three factors, which are the electron affinity (EA) of acceptor, the ionization potential (IP) of donor and the electrostatic Coulomb forces between D-A pairs.[39] Since the first reported case in 1967, CT cocrystal materials have shown different functions, involving high conductivity in room temperature, superconductivity in high temperature, ambipolar transport,

ferroelectricity, magnetism and photoconductivity.[28,40] On the other hand, strong π-π interaction triggers the self-assembly between π-donor (such as porphyrin) and π-acceptor (such as fullerene) in the crystalline state.[41] For instance, DPTTA–C60,[13] one typical cocrystal formed by strong π-π stacking, displayed the excellent ambipolar charge-transport mobility. Because of the robust stability (especially triple or quadruple hydrogen bond) and the clear orientation, hydrogen bond plays an important role for designing organic cocrystals.[2] Hydrogen bonds can not only control the final structure of cocrystal, but also is closely related to their functions.[42,43] For instance, by a lock-arm supramolecular ordering (LASO) strategy, pyromellitic diimide-based cocrystal was successfully synthesized.[44] With the cooperative effect of CT interaction and hydrogen bond, this cocrystal showed the firm structural stability, room-temperature ferroelectric polarization switching[45] and two-axes ferroelectric polarization.[46] Halogen-bond (Scheme 1) is similar to hydrogen bond, which is one noncovalent interaction between donor (halogen atom) and acceptor (nucleophilic region).[28,47-49] Except for the properties similar to those of hydrogen-bond, halogen-bond also can exhibit hydrophobic character and be more feasible at supramolecular self-assembly than hydrogen-bond. Moreover, such cocrystals showed the promising emissive, conductivity, and magnetic properties.[3,4] Actually, because the cocrystal formation is usually triggered by the simultaneous cooperation of different noncovalent interactions, studying the relevance between cooperatively noncovalent interaction and property may assist the arrangement of cocrystals according to the established design.

Up to now, three main strategies applied for co-crystallization, including vapor phase (Figure 1a),[36] liquid phase (Figure 1b)[50] and solid phase (mechanochemical, commonly grinding).[25,26] In comparison with vapor-phase or solid-phase methods, the solution-based technique is more popular, because of its convenience, low cost and versatility. Several liquid-phase techniques were explored, including liquid/liquid interfacial precipitation,[51] solvent-vapor annealing,[52] reprecipitation,[50] drop-casting and diffusion. Certainly, this method is more suitable for the co-crystallization of planar molecules with similar solubility.[53] Although the cases prepared by vapor-phase method were seldom,[36] this strategy was friendly for the co-crystallization of organics with poor solubility, especially insoluble molecules with similar sublimation points.[28,54-56] In solid-phase methods, comparing to traditional grinding, liquid-assisted grinding (LAG) was more efficient.[25,26]

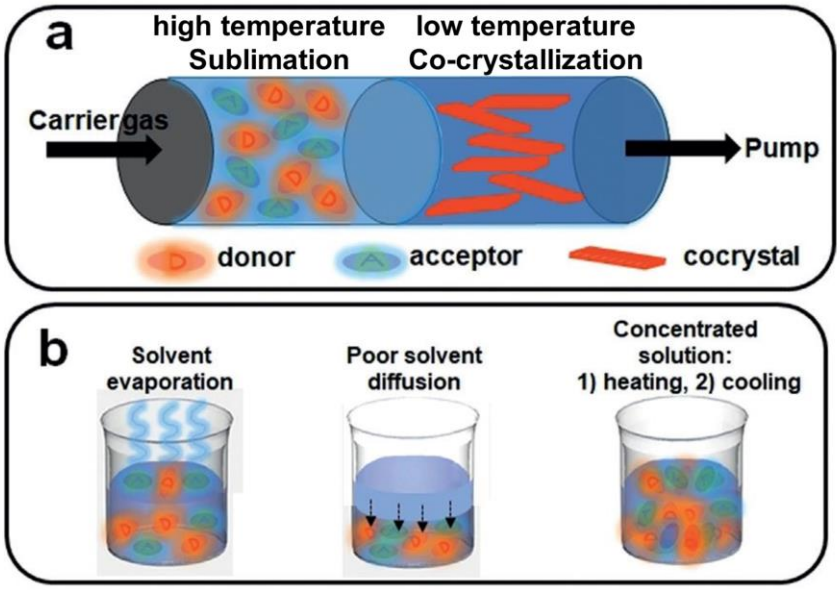

Figure 1. Common preparations methods (a: vapor phase, and b: liquid phase). Adapted with permission from Ref. [4]. Copyright (2019) WILEY-VCH Verlag GmbH & Co. KGaA, Weinheim.

3. LUMINESCENT ORGANIC COCRYSTALS

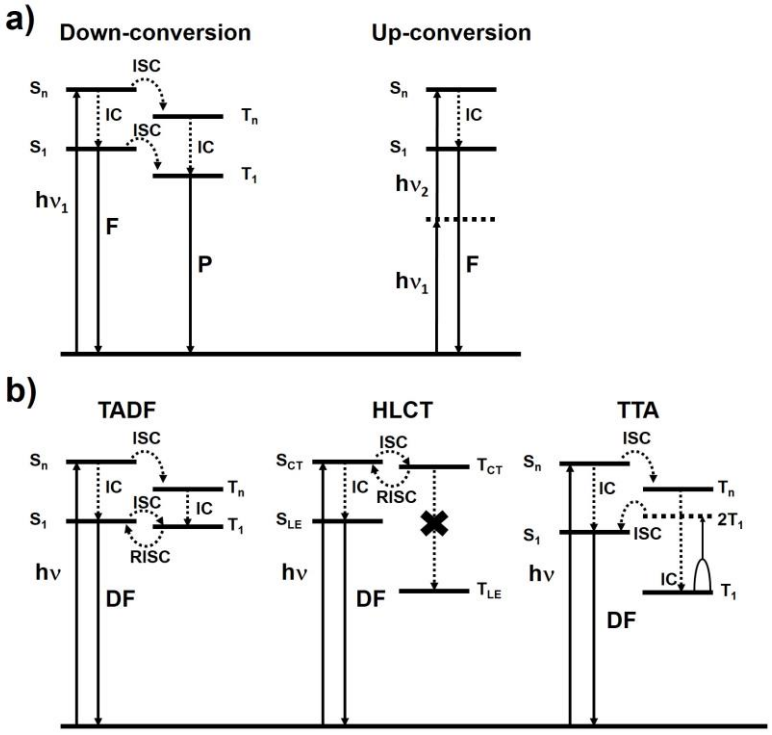

Scheme 2. Jablonski diagrams showing the main mechanisms of luminescent phenomena. a) Process diagrams for fluorescence and phosphorescence. b) Process diagrams for thermally activated delayed fluorescence (TADF), hybridized local and charge transfer (HLCT) and triplet-triplet annihilation (TTA). (IC: internal conversion; ISC/RISC: intersystem crossing or reversed intersystem crossing.)

Generally, luminescent materials can emit light by the conversion of excitation energy, mostly of which are in the visible and near infrared (NIR) regions. The luminescence are caused by the excitation energies from different origins, including a chemical reaction (chemiluminescence), passing an electric current through a substance (electroluminescence), a mechanical action (mechanoluminescence), or absorbing photons (photoluminescence). In this part, based on organic cocrystals, we will cover photoluminescence (hereafter luminescence) and photoluminescent (hereafter luminescent) materials. As we know, luminescent material can show the down-conversion emission with positive Stokes' shift, while up-conversion emissions with negative Stokes' shifts are observed in some of them (commonly two-photon emission). At the same time, luminescence also is divided into fluorescence and phosphorescence, according to the nature of the excited state. Significantly, except for ultralong phosphorescence, there are several organic afterglow phenomena, such as thermally activated delayed fluorescence (TADF), hybridized local and charge transfer (HLCT) and triplet-triplet annihilation (TTA). The mechanisms of those phenomena are briefly illustrated by Jablonski diagrams shown in Scheme 2. Up to now, through this facile cocrystal engineering way, many well-designed optical materials were obtained for different purposes,[3,4,57-59] the emission properties of which were effectively modulated, including color (Figure 2), quantum yield, chirality and lifetime.

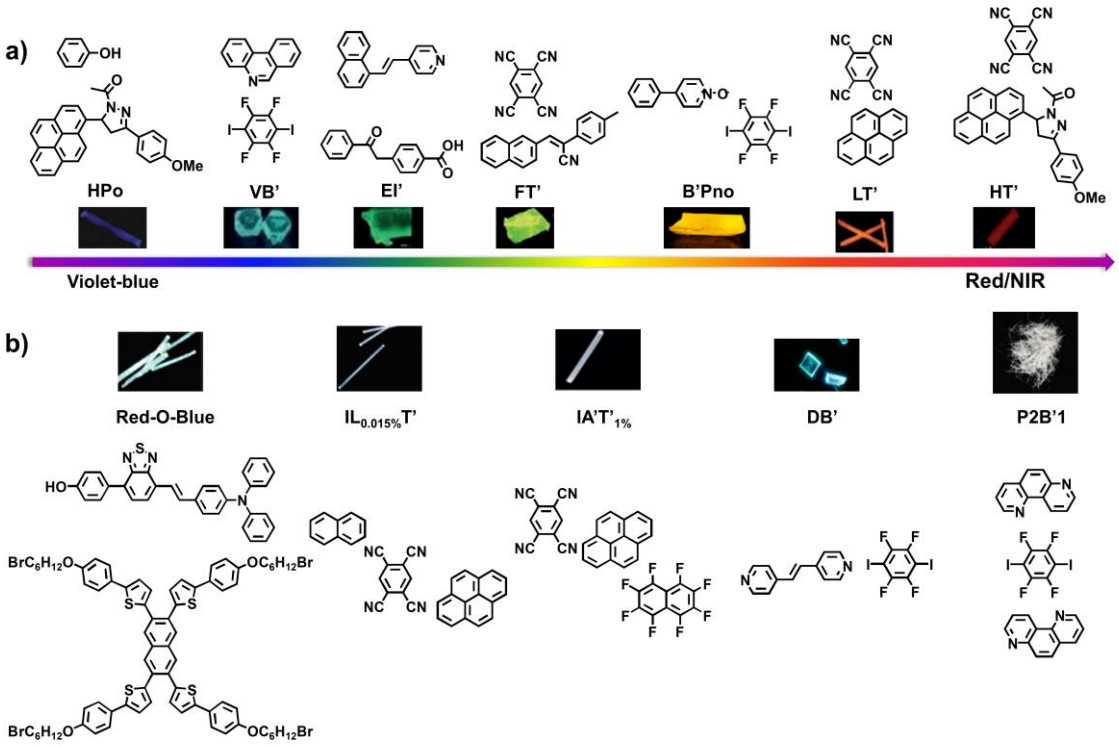

Figure 2. a) Fluorescence microscopy images of cocrystal examples with different color emission in visible range. b) Fluorescence microscopy images of cocrystal examples with white light emission. Adapted with permission from Ref. [50,53,57-64]. Copyright (2015, 2018, 2010, 2017) American Chemical Society, (2012, 2018, 2017, 2019) Wiley-VCH, and (2013, 2014) the Royal Society of Chemistry, respectively.

Haloperfluorobenzene (such as B': 1,4-diiodotetrafluorobenzene; C': 1,4-dibromotetrafluorobenzene) was a good choice to construct versatile cocrystals. When another component fluorescent cyanostilbene (CS) or 1,2-bis(4-pyridyl)ethylene (Bpe, D), was co-assembled to form cocrystal by hydrogen/halogen bonding, the emission color of related cocrystal could be from violet-blue to green.[11,33,53,65,66] On the other hand, 4-phenylpyridine *N*-oxide (Pno), a typical UV/blue fluorescent emitter in the solid phase, was co-assembled with 1,4-diiodotetrafluorobenzene to obtain one cocrystal (Figure 2, B'Pno) with yellow light CT emission.[57] Interestingly, comparing to no or weak emission in the crystal of related single component, when 3-ring-*N*-heterocyclic hydrocarbons and fluoranthene were co-crystallized with haloperfluorobenzenes, such cocrystal could display different luminescences,[61,67-70] including blue, green (Figure 2, V: phenanthridine, VB'), orange yellow, orange or pink. Tetracyanobenzene (T'), one famous acceptor, was a molecule that could show the bright blue fluorescence.[71] In these cases, the emission color of organic solid materials was easily modulated by CT interactions from green (such as FT', F: 3-(naphthalen-2-yl)-2-(*p*-tolyl)acrylonitrile) to red (such as HT', H: 2-(4-methoxyphenyl)-3-(pyren-1-yl)acrylonitrile) range, not only for two component complexes[21,59,72] but also for three component complexes.[50,63,73] Significantly, because the typical luminescence of single-component and/or CT complex was maintained by controlling the ratio of each component in related organic cocrytal, white-light emitting (WLE) was also discovered by several research groups, such as Red-o-Blue (Red-OH: (*E*)-4-(7-(4-(diphenylamino)styryl)benzo[*c*][1,2,5]thiadiazol-4-yl)phenol, Blue-Br:
2-(3,6,7-tris(5-(4-(6-bromohexyloxy)phenyl)thiophen-2-yl)naphthalen-2-yl)-5-(4-(6-bromohexyloxy)-phenyl)thiophene),[60] $IL_{0.015\%}T'$ (I: naphthalene, L: pyrene),[50] $LA'T'_{1\%}$ (A': octafluoronaphthalene),[63] DB'[53] and P2B' (P: 1,7-phenanthroline).[64]

Comparing to molecule in diluted solution or restricted in the host, the bulk properties in solid were more difficult to predict or control, which were strongly altered by the subtle interplay of molecular orientation/arrangement in the condensed phase. Because strong intermolecular interaction was a double-edged sword, to obtain single-component organic luminescent solid material with high quantum yield could be a hard task. For instance, although larger intermolecular π-overlaps in combination with larger transfer integrals (like H-aggregation) and lower reorganization energy result in better electronic properties,[1,74] the strong electronic coupling with H-aggregation in these cases often leads to seriously quenched emissive state with a hypsochromic shift. Therefore, different from efficient non-irradiation decay of non-planar molecule in solution by free rotation and/or vibration, such molecule in solid state (aggregation-induced effect) can just avoid the strong electronic communication caused by too strong intermolecular forces to show bright luminescence, because of the non-planar structure nature. However,

this personality has also caused most of AIE-active organic molecules to be multifunctional only through complex synthesis, not more convenient crystal engineering.

Recently, a technology based on multicomponent systems has been developed to prepare efficient luminescent materials.[75-79] For example, when the 1,3,6,8-tetramethylpyrene (TMPY, pyrene derivative) was doped with perylene, the photoluminescence quantum yield (PLQY) was obviously enhanced by the energy transfer.[80] Recently, octafluoronaphthalene (A') with a high band energy gap (ca. 3.78 eV) was used as a molecular barrier to improve the solid-state emission of polycyclic aromatic hydrocarbon (PAH) chromophores, such as coronene (2.76 eV) and anthracene (3.10 eV). This molecular barrier could be intercalated in to form a periodic π-stacked molecular complex, which effectively blocked the interaction and electron exchange between the two adjacent fluorophores as well as the ISC (Figure 1a) process. Hence, the PLQYs of such cocrystals were extremely increased.[77] Furthermore, 9,10-diphenylanthracene (DPA) was a high ECL efficiency in solution but much lower efficiency in device, whereas the ECL signal of corresponding cocrystal was greatly improved, because the enhanced donor-acceptor and π-π stacking interactions could accelerate electron transfer.[79]

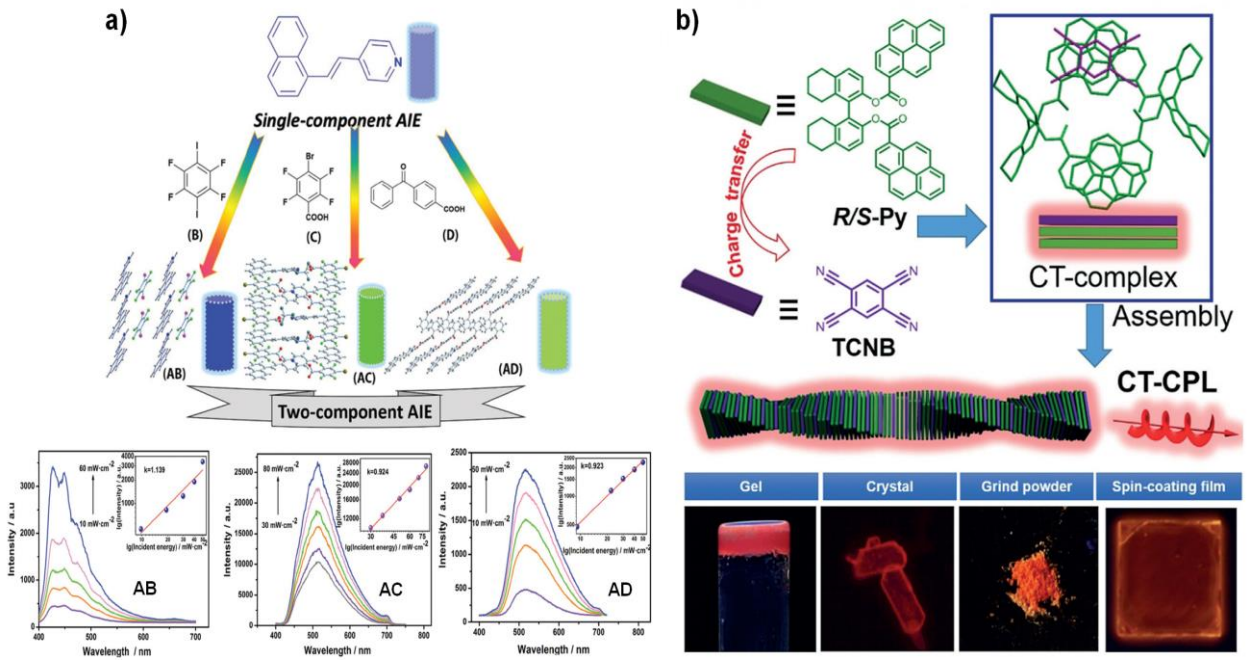

Figure 3. a) Illustration of cocrystal examples showing two-photon fluorescence with different color (**A**: 4-(1-naphthylvinyl)pyridine; **B**: 1,4-diiodotetrafluorobenzene; **C**: 4-bromotetrafluorobenzoic acid; **D**: 4-benzoylbenzoic acid). b) Illustration of chiral CT complexes obtained by blending chiral R/S-Py with achiral acceptor TCNB displaying intense CPL. Adapted with permission from Ref. [58, 10]. Copyright (2018, 2019) WILEY-VCH Verlag GmbH & Co. KGaA, Weinheim.

In 2018, Yan and co-workers reported one interesting example of two-photon fluorescent cocrystals.[58] Comparing to no two-photon fluorescence in pristine (naphthylvinyl)pyridine solid, the cocrystal (Figure 3a) presented the adjustable two-photon fluorescence, which might be originated from its CT complex structure to enhance nonlinear absorptive cross section. More recently, Duan and coworkers designed and prepared a chiral CT system consisting of chiral electron donor and achiral electron acceptor that showed bright CPL with large glum value (Figure 3b). These complexes were fabricated by π-π stacking and strong CT interactions to enable the CPL activity by the large magnetic dipole transition moment.[10]

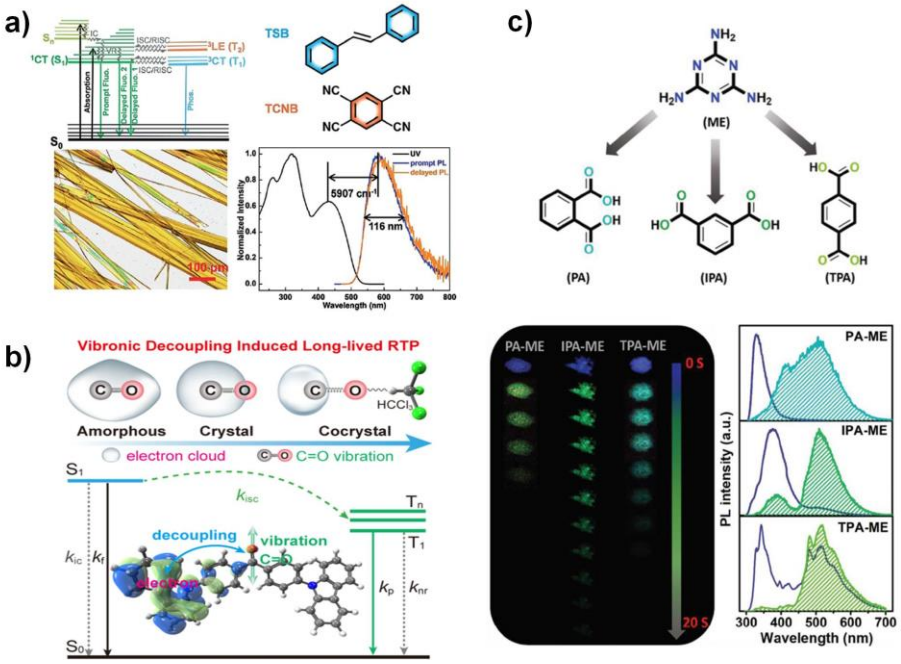

Figure 4. a) Illustration for the cocrystal example showing TADF behavior. b) Illustration for the mechanism of cocrystal example showing long-lived organic room-temperature phosphorescence. c) Illustration for cocrystal example showing phosphorescent afterglow. Adapted with permission from Ref. [81-83]. Copyright (2019) American Chemical Society, (2019) WILEY-VCH Verlag GmbH & Co. KGaA, Weinheim.

Molecular material with long-lived excited state that can exhibit the delayed fluorescence or room-temperature phosphoresce (RTP) has attracted extensive attention in various fields including optical imaging, display device and sensor.[84,85] In this area, although the exploration of such organic cocrystal material is still in the early stages of development, there are several current reports that show the amazing possibilities.[14,64,81-83,86-89] As shown in Figure 4a, Hu and coworkers reported that TADF was observed in a molar ratio of 1:2 CT cocrystal complex of *trans*-1,2-diphenylethylene (TSB) and TCNB (B'), because intermolecular CT in cocrystal with narrowe singlet-triplet energy gap (ΔE_{ST}) was indicated to facilitate the RISC. This work opening a new window for the further design and preparation of novel TADF materials.[83] In the same year, two groups explored cocrystal engineering method to achieve ultralong RTP

in luminescent organic material, respectively. For instance, Shuai and co-workers found that the strong intermolecular hydrogen bonds (C=O···H−C) between 4,4'-bis(9H-carbazol-9-yl)methanone (Cz2BP) and chloroform in cocrystal decreased the nonradiative-decay-rate of $T_1 \rightarrow S_0$ by the vibronic decoupling effect on the C=O stretching motion as well as increased the ($\pi\pi^*$) composition in the T_1 state of Cz2BP (Figure 4b). Hence, such cocrystal emitted the bright ultralong RTP with a lifetime of 353 ms.[81] This novel understanding showed a new strategy to design organic RTP materials. On the other hand, Yan group designed a TADF-assisted energy transfer route to achieve the enhancement of persistent luminescence with an RTP lifetime as high as 2 s.[82] The energy transfer donor and acceptor species were based on the TADF (ME) and RTP (PA, IPA andor TPA) molecules, which were self-assembled into two-component cocrystals by hydrogen-bonding interactions. In these cases, the efficiency of Förster resonance energy transfer (FRET) between donor and acceptor were as high as 76%. Moreover, such cocrystal materials displayed the potential application for information security and personal identification systems.

4. APPLICATION OF ORGANIC COCRYSTAL IN OLET AND LASING

As we all know, one of the most significant applications of CT organic cocrystal is to use it as an new-type ambipolar transporting semiconductors.[13,90] In these cases, molecular orbital interaction could afford efficient electronic coupling both for holes and electrons through superexchange process.[91,92] Hence, such D-A system with characteristic CT luminescence also could imply potential application of organic light-emitting transistor (OLET) based on the combined transport and emission properties. In 2017, Park and coworkers designed a novel 2D-type slab crystal based on CT organic cocrystal (donor : acceptor = 2:1) (Figure 5) to explore its potential application in OLET.[93] In supermolecular synthetic process of such cocrystal with a peculiar quasi-2D arrangement, except for Coulombic CT interaction, side-by-side cyano group induced dipole interaction (Figure 5b) as well as π-π stacking were also the important driving forces. Interestingly, balanced ambipolar transport (μ_e, $\mu_h \approx 10^{-4}$ cm^2 V^{-1} s^{-1}) and bright luminescence ($\Phi_F \approx 60\%$) were the robust support in organic field-effect transistor (OFET) device of such cocrystal to achieve the first CT organic light-emitting transistor with high external quantum efficiency of 1.5%.

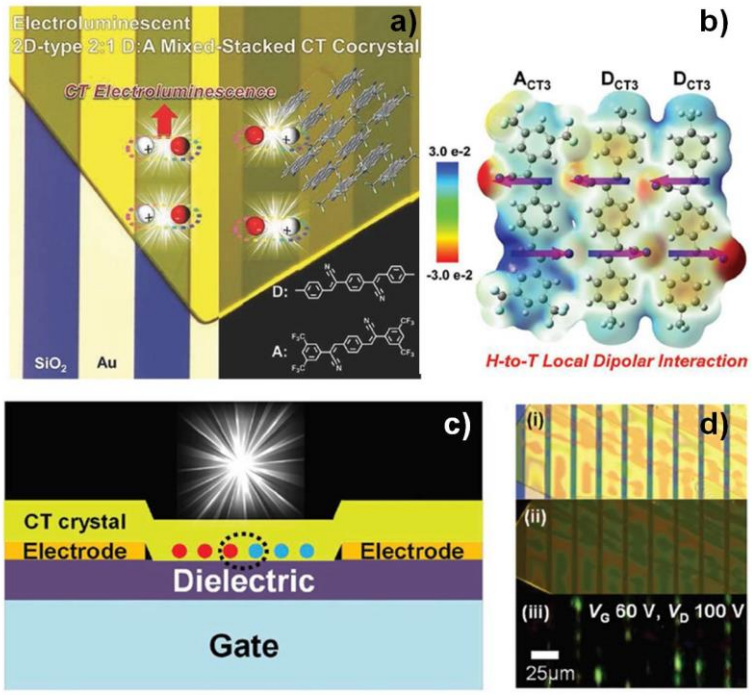

Figure 5. a) Illustration of CT cocrystal for the SC-OLET device. b) DFT-calculated electrostatic potential map to manifest head-to-tail dipolar interaction. c) SC-OLET device structure diagram based on the bottom-contact configuration. d) Images of a device; taken by optical microscopy under white light irradiation (i) and UV irradiation (ii). (iii) was captured during device operation (constant bias condition, V_G: 60 V, V_D: 100 V). Adapted with permission from Ref. [93]. Copyright (2017) WILEY-VCH Verlag GmbH & Co. KGaA, Weinheim.

In laser device, microcrystal can be the optical and/or laser resonator, the crystalline facet of which acts as feedback mirror. On the other hand, the generated photons can be confined in the crystal by internal reflection.[94-96] Especially, π-conjugated molecule microcrystal often offers the advantage of semiconducting property and the possibility of controlling shape, molecular order and orientation by simple crystallization process. Because FRET was a facile way to harvest light and transfer it from an energy donor (D) to an acceptor (A) molecule, FRET-assisted lasing from solid microcrystalline resonators composed of organic molecules would be expected to obtain lasing action with high efficiency. In 2018, Yamamoto and co-workers reported the first example in this area, which was fabricated by a mixture of carbon-bridged oligo(*p*-phenylenevinylenes) (COPVs, Figure 6a).[22] In this case, two COPVs self-assembled forming micrometer-sized, faceted co-crystals with a variety of the mixing ratio, and the lasing wavelength could be tuned by the doping amount of A (Figure 6b). As shown in Figure 6c, lasing occurred with single- and dual vibronic levels. Upon weak excitation of the single D-A cocrystal (below P_{th}), FRET occurred to exhibit spontaneous emission from A. Oppositely, stimulated emission was dominant upon strong pumping (above P_{th}) to generate lasing action from D. Time-resolved spectroscopic studies reveal that the rate constant of lasing is more than 20 times greater than that of FRET (Figure 6c). Furthermore, while the cocrystals were vertically grown on a Ag-coated substrate, it reduced the lasing

threshold by one-fourth. This study showed a possible direction toward organic solid FRET lasers with microcrystalline resonators.

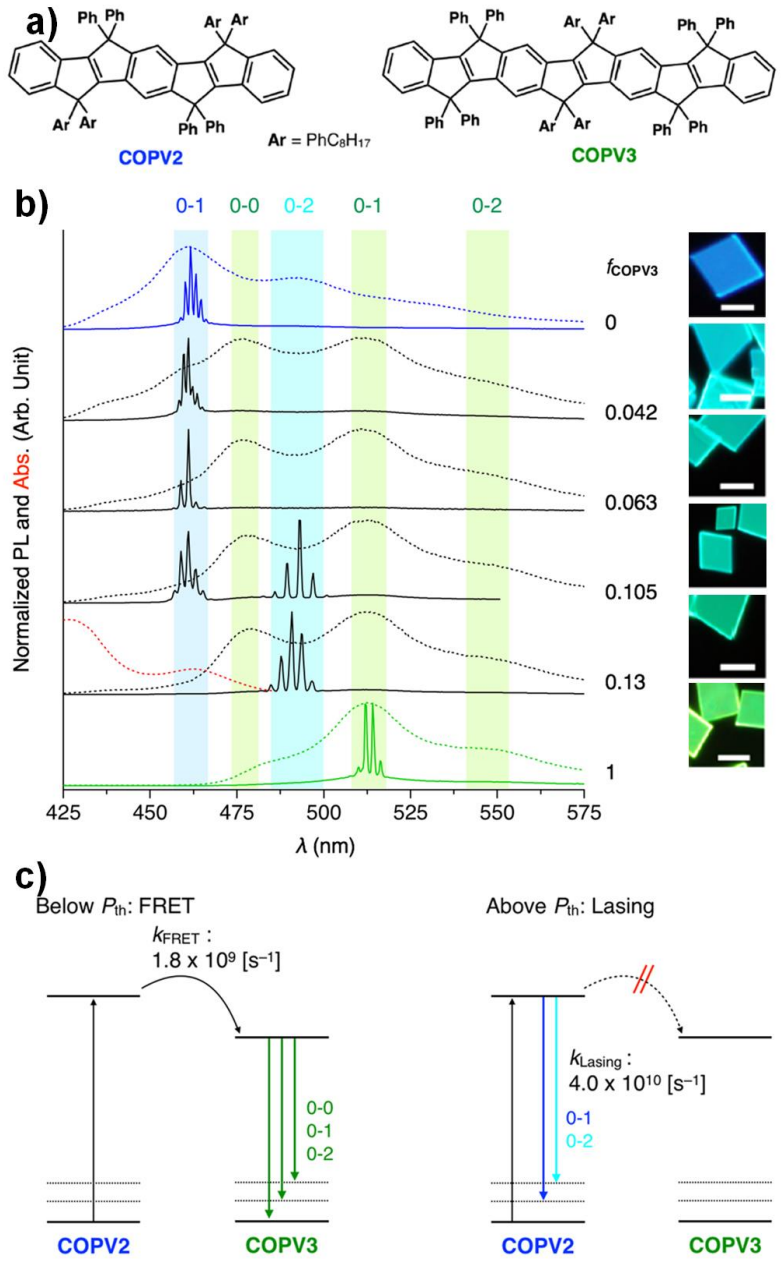

Figure 6. a) The structural formula of **COPV2** and **COPV3**. (b) PL spectra of a single microcrystal of **COPV2** and **COPV3** with f_{COPV3} = 0 (blue), 0.042-0.13 (black), and 1 (green) upon femtosecond excitation with weak pumping below P_{th} (broken curves) and strong pumping above P_{th} (solid curves). Red broken curve indicate photoabsorption spectrum of the co-crystal with f_{COPV3} = 0.13. Inset: Fluorescent micrographs of microcrystals of **COPV2**, **COPV3** and cocrystals. c) Schematic representations of the energy level diagram and emission mechanism upon excitation below and above P_{th}. Adapted with permission from Ref. [22]. Copyright (2018) American Chemical Society.

5. APPLICATION OF ORGANIC COCRYSTAL IN NONLINEAR OPTICAL AND OPTICAL WAVEGUIDE MATERIAL

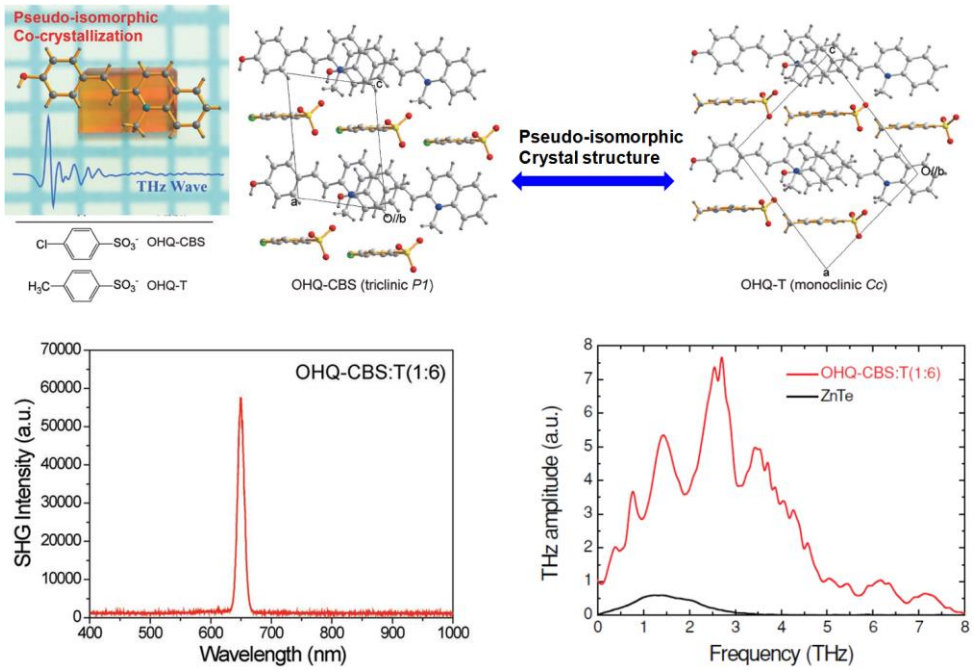

Figure 7. Illustration of cocrystal for THz generation (OHQ-T crystal and OHQ-CBS crystal exhibited pseudo-isomorphic crystal structures, respectively.). Inset: SHG and THz signal of OHQ-CBS:T (1:6) cocrystal at a fundamental wavelength of 1300 nm. Adapted with permission from Ref. [100]. Copyright (2018) WILEY-VCH Verlag GmbH & Co. KGaA, Weinheim.

Generally, with low-cost, simple processing, light-weight and the versatility of synthetic methods, organic nonlinear optical (NLO) materials is helpful in the field. As the nonlinearity it takes that the dielectric polarization P responded to the electric field E of the light, high-polar molecule commonly was the favorable candidate for NLO material. Furthermore, suitable crystallization strategy is considerable in designing and developing novel NLO materials. For example, as the current and necessary energy-conserved process, second harmonic generation (SHG) transfers the light with the incident frequency (ω) into radiation with twice frequency (2ω).[97] Because the asymmetric structure is essential for SHG crystalline material, SHG properties could be modulated by introducing additional components in cocrystal engineering. At recent time, Hu group demonstrated that the SHG property of SPE molecule was owing to the D-A configuration with intramolecular electronic polarization being centrally asymmetric, while centrosymmetric Spe–F4DIB cocrystal showed no SHG property.[98] Yan group reported that the pristine 2,5-diphenyloxazole (DPO) shows no SHG behavior but up-conversion emission, however, the noncentrosymmetric cocrystals could show the SHG performances.[99] In 2018, Kwon and co-workers reported a new organic three-component single crystals, which is produced from so-called "pseudo-isomorphic cocrystallization" applied into the nonlinear optical and terahertz (THz) photonic

(Figure 7). The new organic cocrystals are applied for varies of optical experiments with the advantages of large macroscopic optical nonlinearity, excellent optical quality and morphology, which is consist of highly nonlinear optical 2-(4-hydroxystyryl)-1-methylquinolinium (OHQ) cation, and two different counter anions (CBS and T). The OHQ-based cocrystal presented a broad spectral bandwidth of up to 8 THz, who delivered one order of magnitude higher peak-to-peak THz electric field than the standard ZnTe crystal.[100]

Two-photon absorption (TPA) material has showed the appealing applications in varies of fields in third-order NLO area, such as 3D fluorescence imaging, optical data storage, lasers, optical limiting, and lithographic microfabrication. Besides, organic cocrystals with a clear structure play an important and demonstrating role in revealing the intrinsic properties of a multicomponent system. For example, although the TPA properties of stilbene derivatives have been extensively studied in the liquid state,[104] solid-state stilbene-type material with TPA performance is rare. In 2017, Hu group explored a cocrystal strategy to yield TPA properties in stilbene-type cocrystals.[105] The Spe–TCNB cocrystals exhibited the unique TPA property comparing to that of the constituent units, because of intermolecular charge-transfer (ICT) interactions in the D-A system.

Recently, there are some reviews about the detail of organic optical waveguide cocrystals.[3,4,30] In this section, we will briefly make an introduction to the development of this area. Because such 2D material can transfer photon along different direction, it is extremely suitable for the preparation of optical planar diodes,[106,107] whispering-gallery-mode (WGM) resonator[108,109] and organic crystal lasing.[110] In comparison with organic molecules present 2D self-assembly behaviors for a single component material,[111] several groups reported that the structures of 2D multi-component optical waveguide cocrystals were conveniently tuned by anisotropic noncovalent interactions (hydrogen/halogen bonds and/or D-A interactions).[98,112,113] Furthermore, some of 2D cocrystals could be presented as a micro optical logic gate containing multiple input/out channels based on their packing direction-oriented asymmetric photon transport, which might provide potential applications of the 2D cocrystals for the integrated organic photonics.

6. APPLICATION OF ORGANIC COCRYSTAL IN STIMULI-RESPONSIVE MATERIAL AND OTHER POTENTIAL APPLICATIONS

Because of stimuli-active component as well as the sensitive noncovalent interaction between components,[11,114] cocrystals assembled from multiple components can be a favorable platform to switch and modulate the bulk properties by external perturbations.[115-117] For example, in the review paper written by Zhang *et al.*,[4] the authors introduced some attractive reports, in which the luminescence and/or shape of cocrystals could be finely turned by external perturbations. These results may lead to applications in

electronic display and information storage systems, smart sensors/switches, optical switching devices and memory devices. Herein, we will introduce two interesting literatures as the complement. In 2019, Hisaeda and co-workers designed three crystals, salts/cocrystals/salt-cocrystal continuum, the structure-property relationships of which were well studied to realize the regulation of proton transfer dynamics between acid-base (AB) complexes by photoluminescent color changes (Figure 8). The extent of proton transfer in the acid-base complexes consisting of a pyridine-modified pyrrolopyrrole dye and organic acids (Figure 8a) would be determined by the Δp*Ka* value and crystalline environment.[118] Furthermore, the extent of proton transfer would govern the ICT strength of AB complexes and tune the luminescence (Figure 8b). Because enhancing ICT strength leaded to a red-shifted emission from blue to yellow under UV light, the salt-cocrystal continuum (Figure 8c) showed vapochromism against CH_2Cl_2.

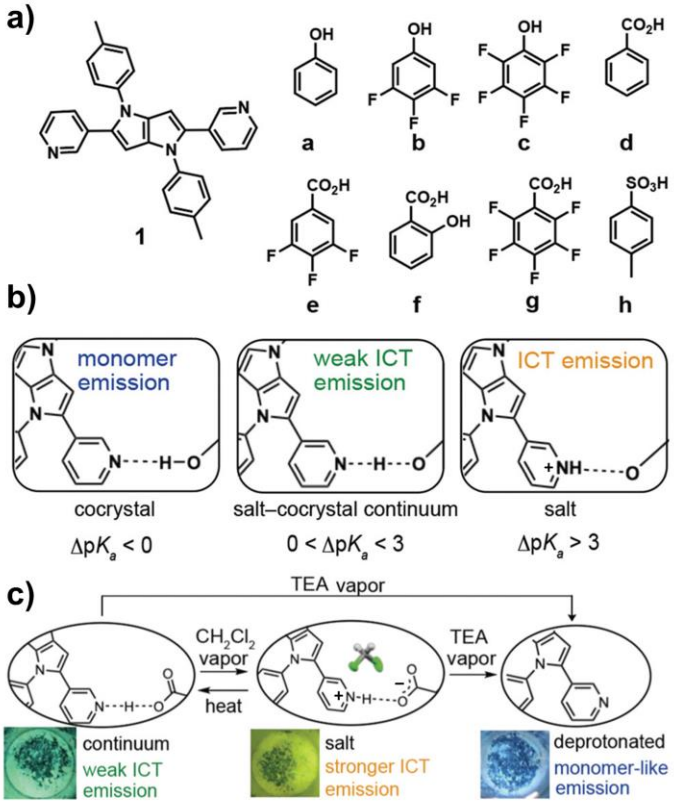

Figure 8. a) The structural formula of the cocrystal motifs. b) The mechanism of photofunction modulation was effected by the strength of ICT. c) Schematic representation of emission color changes caused by external stimuli. Adapted with permission from Ref. [118]. Copyright (2019) the Royal Society of Chemistry.

Prominent piezochromic materials play a vital role in the development of damage detection devices and smart sensors. However, compared to other external stimuli (such as light, pH and temperature), the investigation to understand intermolecular interactions and piezochromic properties based on

multicomponent molecular hybrid materials was still limited. In 2018, Yang and co-workers choose 4-bis(1-cyano-2-phenylethenyl)benzene (DCSB, A) as the core chromophore to assemble with two small organic molecules (tetrafluorohydroquinone (B) and 2,3,5,6-tetrafluoro-4-hydroxybenzoic acid (C)), for studying the relationship between solid-state molecular arrangement and piezochromic behavior (Figure 9). With the specific environmental stimuli (applied pressure and vapor fumigation), the co-crystals exhibited prominent piezochromic properties and fluorescence quenching phenomena due to the collapse of inner supramolecular architectures.[119]

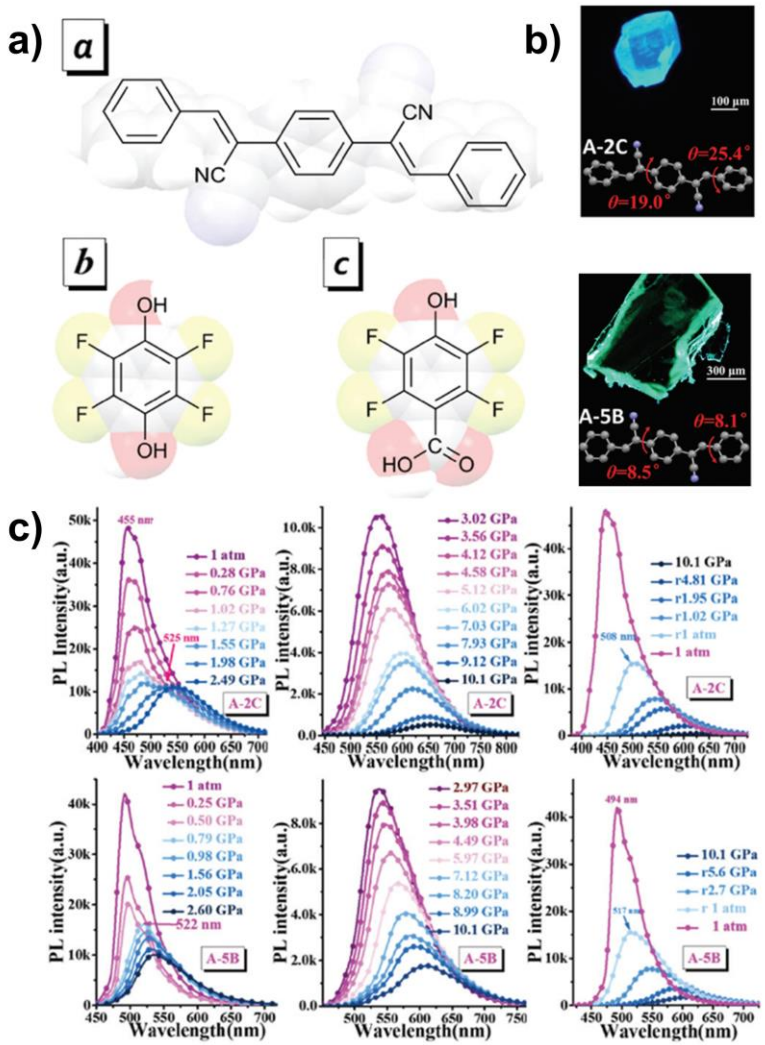

Figure 9. a) Molecular cocrystals of DCSB-derivatives with two small organic molecules. b) Fluorescence images and dihedral angles between intermediate benzene ring and bilateral benzene rings of DCSB-base cocrystals **A-2C** and **A-5B**. (c) In situ PL spectra of cocrystals **A-2C** and **A-5B** under pressure in the range 1 atm~10 GPa. Adapted with permission from Ref. [119]. Copyright (2018) the Royal Society of Chemistry.

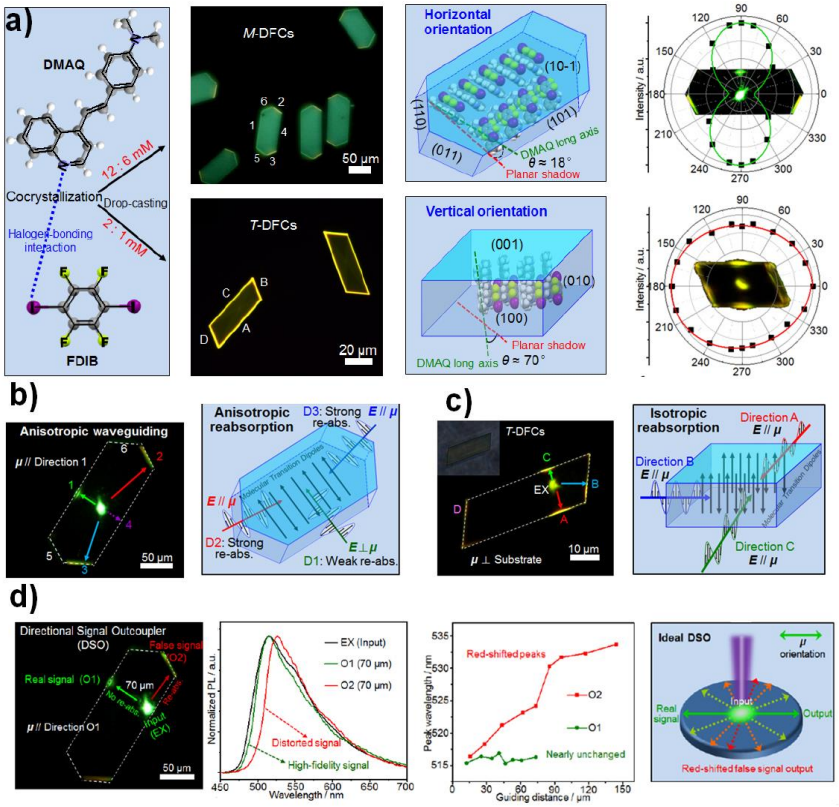

Figure 10. a) Molecular structure of each component, PL image, molecular orientation, incident-polarization-angle-dependent PL intensity for the monoclinic (*M*-DFC) or triclinic (*T*-DFC) cocrystals, respectively. b) PL images of *M*-DFC excited by polarization perpendicular (focused 400 nm laser) to the width direction, and illustration for the direction-dependent re-absorption waveguiding loss mechanism. c) PL and bright-field (inset) images of a *T*-DFC excited with the 400 nm laser beam focusing at the center and the drawing reveals the direction-independent re-absorption waveguiding loss mechanism. d) PL image of a 2D M-DFC waveguide with different output directions but the same propagation distance defining a DSO; spatially resolved micro-PL spectra collected from the EX, O1 and O2; plot of outcoupled signal peaks against guiding distance from O1 and O2, respectively; and illustration of an ideal DSO device. Adapted with permission from Ref. [120]. Copyright (2020) WILEY-VCH Verlag GmbH & Co. KGaA, Weinheim.

The two-dimensional (2D) anisotropic transmission of photons and electrons is particularly important in the construction of ultra-compact on-chip circuits. The photons in organic 2D crystals usually exhibit the isotropic propagation, however, the anisotropic behaviors have not yet been fully demonstrated. Very recently, Zhao and co-workers explored an orientation-controlled photon-dipole interaction strategy to rationally realize the anisotropic and isotropic 2D photon transmissions in two cocrystals (Figure 10).[120] In this case, The monoclinic microplate M-DFC that adopted a nearly horizontal molecular transition dipole orientation in the 2D plane, exhibited the distinct re-absorption waveguide losses for different 2D directions by anisotropic photon-dipole interaction (Figure 10b). In contrast, because the triclinic microplate T-DFC showed a vertical transition dipole orientation, the 2D isotropic photon-dipole interactions in this cocrystal triggered the same re-absorption losses along different directions (Figure

10c). In this literature, the authors designed a directional signal outcoupler (DSO) for the high-fidelity transmission of the real signals, which would enlighten the development of 2D anisotropic optical devices (Figure 10d).

In addition to the above research, organic cocrystals possesses some other characteristics, like near-infrared photothermal conversion and imaging of DBTTF-TCNB cocrystal[24] and emission-sensitive cocrystal GD2DNS for nitroaromatic explosive (trinitrotoluene, picric acid and *m*-dinitrobenzene).[121]

7. CONCLUSIONS

As one emerged star in organic solid materials, organic cocrystals based on noncovalent intermolecular interactions have currently attracted much attention because of their versatile properties and applications. In this short review, we briefly introduced the basis of organic cocrystal and their tunable luminescence performances. Furthermore, we focus on recent researches into organic cocrystals on attractive optical applications, including OLET, lasing, NLO material, optical waveguide, stimuli-responsiveness and 2D anisotropic transport material. However, there are many challenges and opportunities in this new domain. Firstly, there is still a long way to explore the basic interaction mechanism and principles of co-crystallization processes. It is very important for the rational selection of appropriate components as well as the suitably structurally matching, co-assembling, and crystallizing of diverse components in function cocrystals. Subsequently, the effective modulation of cocrystals properties by designing and controlling the definite stoichiometric ratio, molecular stacking mode, orientation, crystal phase and morphology remains at an immature stage. Hence, to achieve functional organic cocrystals, especially material for optofunctional application, need to be further explored. Besides, to find new couples and new components also is essential for researchers in this area, which may bring much fascinating inspiration. We strongly believe that organic cocrystals with excellent prospect will make a big difference in near future.

ACKNOWLEDGEMENTS

The authors acknowledge financial support from the National Natural Science Foundation (No. 21803016), the Science and Technology research projects of colleges and universities in Hebei province (No. ZD2019309), and Excellent Young Fund from Zhengzhou University (No. 1521316017).

REFERENCES

1. X. T. Zhang, H. L. Dong, and W. P. Hu, *Adv. Mater.*, 2018, **30**, 1801048.
2. N. A. Mir, R. Dubey, and G. R. Desiraju, *Acc. Chem. Res.*, 2019, **52**, 2210.
3. L. Sun, Y. Wang, F. Yang, X. Zhang, and W. Hu, *Adv. Mater.*, 2019, **31**, 1902328.

4. Y. Huang, Z. Wang, Z. Chen, and Q. Zhang, *Angew. Chem. Int. Ed.*, 2019, **58**, 9696.
5. R. Davey and J. Garside, Oxford Chemistry Primers. Oxford University Press, New York, 2001.
6. J. Ferraris, D. O. Cowan, V. Walatka, and J. H. Perlstein, *J. Am. Chem. Soc.*, 1973, **95**, 948.
7. S. A. Odom, M. M. Caruso, A. D. Finke, A. M. Prokup, J. A. Ritchey, J. H. Leonard, S. R. White, N. R. Sottos, and J. S. Moore, *Adv. Funct. Mater.*, 2010, **20**, 1721.
8. J. Harada, M. Ohtani, Y. Takahashi, and T. Inabe, *J. Am. Chem. Soc.*, 2015, **137**, 4477.
9. Y. L. Lei, L. S. Liao, and S. T. Lee, *J. Am. Chem. Soc.*, 2013, **135**, 3744.
10. J. Han, D. Yang, X. Jin, Y. Jiang, M. Liu, and P. Duan, *Angew. Chem. Int. Ed.*, 2019, **58**, 7013.
11. D. Yan, A. Delori, G. O. Lloyd, T. Friščić, G. M. Day, W. Jones, J. Lu, M. Wei, D. G. Evans, and X. Duan, *Angew. Chem. Int. Ed.*, 2011, **50**, 12483.
12. R. A. Wiscons, N. R. Goud, J. T. Damron, and A. J. Matzger, *Angew. Chem. Int. Ed.*, 2018, **57**, 9044.
13. J. Zhang, J. H. Tan, Z. Y. Ma, W. Xu, G. Y. Zhao, H. Geng, C. A. Di, W. P. Hu, Z. G. Shuai, K. Singh, and D. B. Zhu, *J. Am. Chem. Soc.*, 2013, **135**, 558.
14. O. Bolton, K. Lee, H. J. Kim, K. Y. Lin, and J. Kim, *Nat. Chem.*, 2011, **3**, 205.
15. Q. J. Shen, H. Q. Wei, W. S. Zou, H. L. Sun, and W. J. Jin, *CrystEngComm*, 2012, **14**, 1010.
16. S. d'Agostino, F. Grepioni, D. Braga, and B. Ventura, *Cryst. Growth Des.*, 2015, **15**, 2039.
17. L. Y. Bai, P. Bose, Q. Gao, Y. X. Li, R. Ganguly, and Y. L. Zhao, *J. Am. Chem. Soc.*, 2017, **139**, 436.
18. G. F. Liu, J. Liu, X. Ye, L. N. Nie, P. Y. Gu, X. T. Tao, and Q. C. Zhang, *Angew. Chem. Int. Ed.*, 2017, **56**, 198.
19. Y. J. Liu, Q. X. Zeng, B. Zou, Y. Liu, B. Xu, and W. J. Tian, *Angew. Chem. Int. Ed.*, 2018, **57**, 15670.
20. P. Gupta, D. P. Karothu, E. Ahmed, P. Naumov, and N. K. Nath, *Angew. Chem. Int. Ed.*, 2018, **57**, 8498.
21. X. Y. Fang, X. G. Yang, and D. P. Yan, *J. Mater. Chem. C*, 2017, **5**, 1632.
22. D. Okada, S. Azzini, H. Nishioka, A. Ichimura, H. Tsuji, E. Nakamura, F. Sasaki, C. Genet, T. W. Ebbesen, and Y. Yamamoto, *Nano Lett.*, 2018, **18**, 4396.
23. S. J. Kang, S. Ahn, J. B. Kim, C. Schenck, A. M. Hiszpanski, S. Oh, T. Schiros, Y. L. Loo, and C. Nuckolls, *J. Am. Chem. Soc.*, 2013, **135**, 2207.
24. Y. Wang, W. G. Zhu, W. N. Du, X. F. Liu, X. T. Zhang, H. L. Dong, and W. P. Hu, *Angew. Chem. Int. Ed.*, 2018, **57**, 3963.
25. D. Braga, L. Maini, and F. Grepioni, *Chem. Soc. Rev.*, 2013, **42**, 7638.
26. T. Friščić, *Chem. Soc. Rev.*, 2012, **41**, 3493.
27. D. Yan and D. G. Evans, *Mater. Horiz.*, 2014, **1**, 46.

28. Y. Wang, W. G. Zhu, H. L. Dong, X. T. Zhang, R. J. Li, and W. P. Hu, *Top. Curr. Chem.*, 2016, **374**, 229.
29. J. Zhang, W. Xu, P. Sheng, G. Zhao, and D. Zhu, *Acc. Chem. Res.*, 2017, **50**, 1654.
30. L. Sun, W. Zhu, F. Yang, B. Li, X. Ren, X. Zhang, and W. Hu, *Phys. Chem. Chem. Phys.*, 2018, **20**, 6009.
31. S. Aitipamula, R. Banerjee, A. K. Bansal, K. Biradha, M. L. Cheney, A. R. Choudhury, G. R. Desiraju, A. G. Dikundwar, R. Dubey, N. Duggirala, P. P. Ghogale, S. Ghosh, P. K. Goswami, N. R. Goud, R. R. K. R. Jetti, P. Karpinski, P. Kaushik, D. Kumar, V. Kumar, B. Moulton, A. Mukherjee, G. Mukherjee, A. S. Myerson, V. Puri, A. Ramanan, T. Rajamannar, C. M. Reddy, N. Rodriguez-Hornedo, R. D. Rogers, T. N. G. Row, P. Sanphui, N. Shan, G. Shete, A. Singh, C. C. Sun, J. A. Swift, R. Thaimattam, T. S. Thakur, R. K. Thaper, S. P. Thomas, S. Tothadi, V. R. Vangala, N. Variankaval, P. Vishweshwar, D. R. Weyna, and M. J. Zaworotko, *Cryst. Growth Des.*, 2012, **12**, 2147.
32. J. Goodman and L. E. Brus, *J. Am. Chem. Soc.*, 1978, **100**, 7472.
33. J. D. Wuest, *Nat. Chem.*, 2012, **4**, 74.
34. J. B. Torrance, *Acc. Chem. Res.*, 1979, **12**, 79.
35. G. D'Avino and M. J. Verstraete, *Phys. Rev. Lett.*, 2014, **113**, 237602.
36. H. T. Black and D. F. Perepichka, *Angew. Chem. Int. Ed.*, 2014, **53**, 2138.
37. R. P. Shibaeva and E. B. Yagubskii, *Chem. Rev.*, 2004, **104**, 5347.
38. A. Das and S. Ghosh, *Angew. Chem. Int. Ed.*, 2014, **53**, 2038.
39. K. P. Goetz, D. Vermeulen, M. E. Payne, C. Kloc, L. E. McNeil, and O. D. Jurchescu, *J. Mater. Chem. C*, 2014, **2**, 3065.
40. T. H. Lee, J. H. Li, W. S. Huang, B. Hu, J. C. A. Huang, T. F. Guo, and T. C. Wen, *Appl. Phys. Lett.*, 2011, **99**, 073307.
41. E. M. Pérez and N. Martín, *Chem. Soc. Rev.*, 2015, **44**, 6425.
42. M. C. Etter, *J. Phys. Chem.*, 1991, **95**, 4601.
43. C. Bosshard, F. Pan, M. S. Wong, S. Manetta, R. Spreiter, C. Z. Cai, P. Gunter, and V. Gramlich, *Chem. Phys.*, 1999, **245**, 377.
44. A. K. Blackburn, A. C. H. Sue, A. K. Shveyd, D. Cao, A. Tayi, A. Narayanan, B. S. Rolczynski, J. M. Szarko, O. A. Bozdemir, R. Wakabayashi, J. A. Lehrman, B. Kahr, L. X. Chen, M. S. Nassar, S. I. Stupp, and J. F. Stoddart, *J. Am. Chem. Soc.*, 2014, **136**, 17224.
45. A. S. Tayi, A. K. Shveyd, A. C. H. Sue, J. M. Szarko, B. S. Rolczynski, D. Cao, T. J. Kennedy, A. A. Sarjeant, C. L. Stern, W. F. Paxton, W. Wu, S. K. Dey, A. C. Fahrenbach, J. R. Guest, H. Mohseni, L. X. Chen, K. L. Wang, J. F. Stoddart, and S. I. Stupp, *Nature*, 2012, **488**, 485.

46. A. Narayanan, D. Cao, L. Frazer, A. S. Tayi, A. K. Blackburn, A. C. H. Sue, J. B. Ketterson, J. F. Stoddart, and S. I. Stupp, *J. Am. Chem. Soc.*, 2017, **139**, 9186.
47. F. J. Guthrie, *J. Chem. Soc.*, 1863, **16**, 239.
48. G. Cavallo, P. Metrangolo, R. Milani, T. Pilati, A. Priimagi, G. Resnati, and G. Terraneo, *Chem. Rev.*, 2016, **116**, 2478.
49. L. Catalano, G. Cavallo, P. Metrangolo, G. Resnati, and G. Terraneo, *Top. Curr. Chem.*, 2016, **373**, 289.
50. Y. L. Lei, Y. Jin, D. Y. Zhou, W. Gu, X. B. Shi, L. S. Liao, and S. T. Lee, *Adv. Mater.*, 2012, **24**, 5345.
51. T. Wakahara, P. D'Angelo, K. I. Miyazawa, Y. Nemoto, O. Ito, N. Tanigaki, D. D. C. Bradley, and T. D. Anthopoulos, *J. Am. Chem. Soc.*, 2012, **134**, 7204.
52. C. Liu, T. Minari, X. Lu, A. Kumatani, K. Takimiya, and K. Tsukagoshi, *Adv. Mater.*, 2011, **23**, 523.
53. W. Zhu, R. Zheng, Y. Zhen, Z. Yu, H. Dong, H. Fu, Q. Shi, and W. Hu, *J. Am. Chem. Soc.*, 2015, **137**, 11038.
54. J. Zhang, P. Gu, G. Long, R. Ganguly, Y. Li, N. Aratani, H. Yamada, and Q. Zhang, *Chem. Sci.*, 2016, **7**, 3851.
55. J. Zhang, G. Liu, Y. Zhou, G. Long, P. Gu, and Q. Zhang, *ACS Appl. Mater. Inter.*, 2017, **9**, 1183.
56. J. Zhang, J. Jin, H. Xu, Q. Zhang, and W. Huang, *J. Mater. Chem. C*, 2018, **6**, 3485.
57. Q. Feng, M. Wang, B. Dong, C. Xu, J. Zhao, and H. Zhang, *CrystEngComm*, 2013, **15**, 3623.
58. S. Li and D. Yan, *Adv. Opt. Mater.*, 2018, **6**, 1800445.
59. R. Usman, A. Khan, M. Wang, Y. Luo, W. Sun, H. Sun, C. Du, and N. He, *Cryst. Growth Des.*, 2018, **18**, 6001.
60. X. Wang, J. Yan, Y. Zhou, and J. Pei, *J. Am. Chem. Soc.*, 2010, **132**, 15872.
61. H. Wang, R. X. Hu, X. Pang, H. Y. Gao, and W. J. Jin, *CrystEngComm*, 2014, **16**, 7942.
62. R. Liu, H. Wang, and W. J. Jin, *Cryst. Growth Des.*, 2017, **17**, 3331.
63. Y. Sun, Y. Lei, L. Liao, and W. Hu, *Angew. Chem. Int. Ed.*, 2017, **56**, 10352.
64. C. Feng, S. Li, X. Xiao, Y. Lei, H. Geng, Y. Liao, Q. Liao, J. Yao, Y. Wu, and H. Fu, *Adv. Opt. Mater.*, 2019, **7**, 1900767.
65. G. Fan and D. Yan, *Sci. Rep.*, 2014, **4**, 4933.
66. J. J. Wu, Z. Z. Li, M. P. Zhuo, Y. Wu, X. D. Wang, L. S. Liao, and L. Jiang, *Adv. Opt. Mater.*, 2018, **6**, 1701300.
67. Q. J. Shen, X. Pang, X. R. Zhao, H. Y. Gao, H. L. Sun, and W. J. Jin, *CrystEngComm*, 2012, **14**, 5027.
68. R. Liu, Y. J. Gao, and W. J. Jin, *Acta Crystallogr. Sect. B*, 2017, **73**, 247.

69. Y. J. Gao, C. Li, R. Liu, and W. J. Jin, *Spectrochim. Acta Part A*, 2017, **173**, 792.
70. L. Li, H. Wang, W. Wang, and W. J. Jin, *CrystEngComm*, 2017, **19**, 5058.
71. I. Shokaryev, A. J. C. Buurma, O. D. Jurchescu, M. A. Uijttewaal, G. A. de Wijs, T. T. M. Palstra, and R. A. de Groot, *J. Phys. Chem. A*, 2008, **112**, 2497.
72. S. Yang, J. You, J. Lan, and G. Gao, *J. Am. Chem. Soc.*, 2012, **134**, 11868.
73. Y. Q. Sun, Y. L. Lei, X. H. Sun, S. T. Lee, and L. S. Liao, *Chem. Mater.*, 2015, **27**, 1157.
74. V. Coropceanu, J. Cornil, D. A. da Silva Filho, Y. Olivier, R. Silbey, and J. L. Bredas, *Chem. Rev.*, 2007, **107**, 926.
75. S. Li, Y. Lin, and D. Yan, *J. Mater. Chem. C*, 2016, **4**, 2527.
76. J. Wang, A. Li, S. Xu, B. Li, C. Song, Y. Geng, N. Chu, J. He, and W. Xu, *J. Mater. Chem. C*, 2018, **6**, 8958.
77. H. Ye, G. Liu, S. Liu, D. Casanova, X. Ye, X. Tao, Q. Zhang, and Q. Xiong, *Angew. Chem. Int. Ed.*, 2018, **57**, 1928.
78. Y. Huang, J. Xing, Q. Gong, L. Chen, G. Liu, C. Yao, Z. Wang, H. Zhang, Z. Chen, and Q. Zhang, *Nat. Commun.*, 2019, **10**, 169.
79. G. Fan and D. Yan, *Adv. Opt. Mater.*, 2016, **4**, 2139.
80. J. Li, S. Takaishi, N. Fujinuma, K. Endo, M. Yamashita, H. Matsuzaki, H. Okamoto, K. Sawabe, T. Takenobu, and Y. Iwasa, *J. Mater. Chem.*, 2011, **21**, 17662.
81. H. Ma, H. Yu, Q. Peng, Z. An, D. Wang, and Z. Shuai, *J. Phys. Chem. Lett.*, 2019, **10**, 6948.
82. B. Zhou and D. Yan, *Adv. Funct. Mater.*, 2019, **29**, 1807599.
83. L. Sun, W. Hua, Y. Liu, G. Tian, M. Chen, M. Chen, F. Yang, S. Wang, X. Zhang, Y. Luo, and W. Hu, *Angew. Chem. Int. Ed.*, 2019, **58**, 11311.
84. S. Xu, R. Chen, C. Zheng, and W. Huang, *Adv. Mater.*, 2016, **28**, 9920.
85. S. Hirata, *Adv. Opt. Mater.*, 2017, **5**, 1700116.
86. H. Y. Gao, X. R. Zhao, H. Wang, X. Pang, and W. J. Jin, *Cryst. Growth Des.*, 2012, **12**, 4377.
87. O. Bolton, D. Lee, J. Jung, and J. Kim, *Chem. Mater.*, 2014, **26**, 6644.
88. T. Ono, A. Taema, A. Goto, and Y. Hisaeda, *Chem. Eur. J.*, 2018, **24**, 17487.
89. S. d'Agostino, F. Spinelli, P. Taddei, B. Ventura, and F. Grepioni, *Cryst. Growth Des.*, 2019, **19**, 336.
90. J. Zhang, H. Geng, T. S. Virk, Y. Zhao, J. Tan, C. Di, W. Xu, K. Singh, W. Hu, Z. Shuai, Y. Liu, and D. Zhu, *Adv. Mater.*, 2012, **24**, 2603.
91. L. Zhu, Y. Yi, Y. Li, E. G. Kim, V. Coropceanu, and J. L. Brédas, *J. Am. Chem. Soc.*, 2012, **134**, 2340.
92. H. Geng, X. Zheng, Z. Shuai, L. Zhu, and Y. Yi, *Adv. Mater.*, 2015, **27**, 1443.

93. S. K. Park, J. H. Kim, T. Ohto, R. Yamada, A. O. F. Jones, D. R. Whang, I. Cho, S. Oh, S. H. Hong, J. E. Kwon, J. H. Kim, Y. Olivier, R. Fischer, R. Resel, J. Gierschner, H. Tada, and S. Y. Park, *Adv. Mater.*, 2017, **29**, 1701346.
94. I. D. W. Samuel and G. A. Turnbull, *Chem. Rev.*, 2007, **107**, 1272.
95. U. Venkataramudu, M. Annadhasan, H. Maddali, and R. Chandrasekar, *J. Mater. Chem. C*, 2017, **5**, 7262.
96. D. Venkatakrishnarao and R. Chandrasekar, *Adv. Opt. Mater.*, 2016, **4**, 112.
97. D. Venkatakrishnarao, Y. S. L. V. Narayana, M. A. Mohaiddon, E. A. Mamonov, N. Mitetelo, I. A. Kolmychek, A. I. Maydykovskiy, V. B. Novikov, T. V. Murzina, and R. Chandrasekar, *Adv. Mater.*, 2017, **29**, 1605260.
98. W. G. Zhu, L. Y. Zhu, L. J. Sun, Y. G. Zhen, H. L. Dong, Z. X. Wei, and W. P. Hu, *Angew. Chem. Int. Ed.*, 2016, **55**, 14023.
99. P. Yan, H. J. Yang, Q. Y. Meng, H. Y. Lin, and M. Wei, *Adv. Funct. Mater.*, 2014, **24**, 587.
100. M. H. Shin, S. H. Lee, B. J. Kang, M. Jazbinšek, W. Yoon, H. Yun, F. Rotermund, and O. Kwon, *Adv. Funct. Mater.*, 2018, **28**, 1805257.
101. F. Terenziani, C. Katan, E. Badaeva, S. Tretiak, and M. Blanchard-Desce, *Adv. Mater.*, 2008, **20**, 4641.
102. M. Feng, H. Zhan, and Y. Chen, *Appl. Phys. Lett.*, 2010, **96**, 033107.
103. Z. Gan, Y. Cao, R. A. Evans, and M. Gu, *Nat. Commun.*, 2013, **4**, 2061.
104. M. Rumi, J. E. Ehrlich, A. A. Heikal, J. W. Perry, S. Barlow, Z. Y. Hu, D. McCord-Maughon, T. C. Parker, H. Röckel, S. Thayumanavan, S. R. Marder, D. Beljonne, and J. L. Brédas, *J. Am. Chem. Soc.*, 2000, **122**, 9500.
105. L. J. Sun, W. G. Zhu, W. Wang, F. X. Yang, C. C. Zhang, S. F. Wang, X. T. Zhang, R. J. Li, H. L. Dong, and W. P. Hu, *Angew. Chem. Int. Ed.*, 2017, **56**, 7831.
106. N. Chandrasekhar and R. Chandrasekar, *Angew. Chem. Int. Ed.*, 2012, **51**, 3556.
107. Z. Zhang, X. Song, S. Wang, F. Li, H. Zhang, K. Ye, and Y. Wang, *J. Phys. Chem. Lett.*, 2016, **7**, 1697.
108. L. Heng, X. Wang, D. Tian, J. Zhai, B. Tang, and L. Jiang, *Adv. Mater.*, 2010, **22**, 4716.
109. Z. Li, M. H. Kim, C. Wang, Z. Han, S. Shrestha, A. C. Overvig, M. Lu, A. Stein, A. M. Agarwal, M. Lončar, and N. Yu, *Nat. Nanotechnol.*, 2017, **12**, 675.
110. H. Mizuno, U. Haku, Y. Marutani, A. Ishizumi, H. Yanagi, F. Sasaki, and S. Hotta, *Adv. Mater.*, 2012, **24**, 5744.
111. R. Dong, M. Pfeffermann, H. Liang, Z. Zheng, X. Zhu, J. Zhang, and X. Feng, *Angew. Chem. Int. Ed.*, 2015, **54**, 12058.

112. Y. L. Questel, C. Laurence, and J. Graton, *CrystEngComm*, 2013, **15**, 3212.
113. M. P. Zhuo, Y. C. Tao, X. D. Wang, Y. Wu, S. Chen, L. S. Liao, and L. Jiang, *Angew. Chem. Int. Ed.*, 2018, **57**, 11300.
114. A. Ciesielski, C. A. Palma, M. Bonini, and P. Samori, *Adv. Mater.*, 2010, **22**, 3506.
115. J. Kunzelman, M. Kinami, B. R. Crenshaw, J. D. Protasiewicz, and C. Weder, *Adv. Mater.*, 2008, **20**, 119.
116. J. Luo, L. Y. Li, Y. Song, and J. Pei, *Chem. Eur. J.*, 2011, **17**, 10515.
117. R. Krishna, M. S. R. N. Kiran, C. L. Fraser, U. Ramamurty, and C. M. Reddy, *Adv. Funct. Mater.*, 2013, **23**, 1422.
118. Y. Yano, T. Ono, S. Hatanaka, D. T. Grykoc, and Y. Hisaeda, *J. Mater. Chem. C*, 2019, **7**, 8847.
119. B. Lu, Y. Zhang, X. Yang, K. Wang, B. Zou, and D. Yan, *J. Mater. Chem. C*, 2018, **6**, 9660.
120. Y. Liu, H. Hu, L. Xu, B. Qiu, J. Liang, F. Ding, K. Wang, M. Chu, W. Zhang, M. Ma, B. Chen, X. Yang, and Y. S. Zhao, *Angew. Chem. Int. Ed.*, 2020, **59**, 4456.
121. D. Yan, Y. Lin, Q. Meng, M. Zhao, and M. Wei, *Cryst. Growth Des.*, 2013, **13**, 4495.

Xiao Han obtained her PhD degree in 2017 from Zhengzhou University. From 2017, she was a lecturer at Handan University. Her main interests are in crystal engineering, small-molecule fluorescent probes, luminescent MOFs.

Linyu Wang received a PhD in Electronic science and technology, at the Xi'an Jiaotong University, where he became lecturer in 2019, at Handan University. His research interest focuses on organic synthesis, nanomaterials, chemiluminescence and fluorescent materials, biosensors.

Gaiqing Xi, professor in Handan University. She received the M.S. degree from the Hebei University in 2004. She used to be a visiting scholar at the Beijing University of Chemical Technology (2010-2011). Currently, she is the dean of College of Chemical Engineering & Material, Handan University. Her interests are in the chemistry of photo-induced C-H bond transformation and surface and interfacial of inorganic and organic materials.